Temperature dependence of working pressure of a nanoporous liquid spring

Yu Qiao,[a] Venkata K. Punyamurtula, and Aijie Han
Department of Structural Engineering, University of California at San Diego, La Jolla, California 92093-0085

Xinguo Kong and Falgun B. Surani
Department of Civil Engineering, University of Akron, Akron, Ohio 44325-3905

(Received 22 August 2006; accepted 15 November 2006; published online 18 December 2006)

The thermal effect on nanofluidic behaviors in a hydrophobic zeolite is investigated experimentally. At a constant temperature, water can be forced to infiltrate into the nanopores as an external pressure is applied and defiltrate as the pressure is lowered, leading to a springlike pressure-volume relationship. As temperature varies, due to the variation in solid-liquid interfacial tension, the infiltration pressure changes significantly. Consequently, the system exhibits a thermally controllable volume memory characteristic, with the energy density higher than that of ordinary shape-memory solids by more than one order of magnitude, providing a promising way for developing high-performance intelligent devices. © *2006 American Institute of Physics*.
[DOI: 10.1063/1.2408664]

While porous materials have been widely applied in chemistry, biology, and energy-related areas,[1] not until recently did their applicability in mechanical systems, particularly intelligent systems, received increasing attention. Based on a theoretical analysis, Laouir *et al.*[2] discussed the energy conversion and dissipation associated with the liquid infiltration and defiltration in a porous network and concluded that it is thermodynamically feasible to develop thermal machines based on surface energy of wetting. The working mechanism is quite straightforward: a nonwetting liquid can be compressed into a porous solid as the external pressure is sufficiently high; as temperature varies, due to the well known thermocapillary effect the solid-liquid interfacial tension would change and thus the liquid can defiltrate as the pressure is maintained constant. In each loading-heating-unloading-cooling cycle, the net output work is[2]

$$W_{\text{net}} = \Delta\sigma \cdot \Delta A, \tag{1}$$

where $\Delta\sigma$ and ΔA are the changes in solid-liquid interfacial tension and area, respectively. It can be seen that, in order to increase W_{net}, the solid-liquid interfacial area must be maximized, making it attractive to use nanoporous materials of ultrahigh pore surface areas, typically in the range of $100-2000\ \text{m}^2/\text{g}$.[3,4] In a nanoporous material based system, for $\Delta\sigma$ around $10-50\ \text{mJ/m}^2$, the specific net output work can be $1-100\ \text{J/g}$, comparable with that of steam engines, which is of great potential for the development of nanometer-scale actuation systems.

The liquid behaviors in nanopores can be very different from that in large channels. One major issue is the possible hysteresis of sorption isotherm; that is, as a nonwetting liquid is forced to infiltrate into a nanopore, it may not come out as the pressure is lowered. This phenomenon has been repeatedly observed in experiments of a number of microporous zeolites[5] and mesoporous silicas,[6–10] the reason of which is still under investigation, probably related to the complicated porous structures,[11] the change in effective contact angle,[12] and the gas phase effects.[13,14] On the other hand, it was discovered that in some other nanoporous materials the hysteresis of liquid infiltration and defiltration was negligible. For instance, Soulard *et al.*[15] noticed that in a zeolite, immediately after the pressure is reduced, the confined liquid would defiltrate; i.e., the defiltration pressure is nearly the same as the infiltration pressure, leading to the springlike volume-pressure relationship.

In the current study, the thermal effect on water infiltration and defiltration in a hydrophobic zeolite is investigated. We attempt to answer the following two questions: (1) whether a nanoporous material of nonhysteretic sorption isotherm can be used to develop thermal nanomachines based on wettability control, and (2) if yes, whether its energy density is sufficiently high.

Figure 1 depicts the experimental setup. The liquid phase was 7 g of de-ionized water, functionalized by 1 g of Zeolyst ZSM-5 zeolite, with the silica/alumina ratio of 280. Prior to the experiment, the zeolite had been dried in air at 150 °C for 12 h. The zeolite had a Mobil-five-type framework, with the cell parameters of $a=20.090$ Å, $b=19.739$ Å, and $c=13.142$ Å. The cell volume was 5211.28 Å^3, and the topological density was $\text{TD}_{10}=960$. It was of a three-dimensional nanoporous structure, with the maximum spherical diameter of 0.63 nm computed based on the Delaunay triangulation. The overall nanopore volume was about 17%.[16]

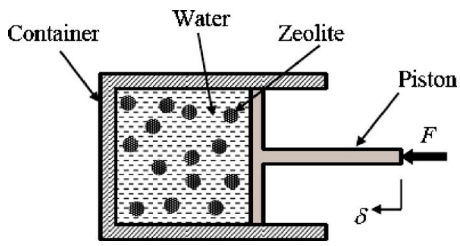

FIG. 1. (Color online) Schematic diagram of the nanoporous material functionalized liquid spring.

[a]Author to whom correspondence should be addressed; electronic mail: yqiao@ucsd.edu

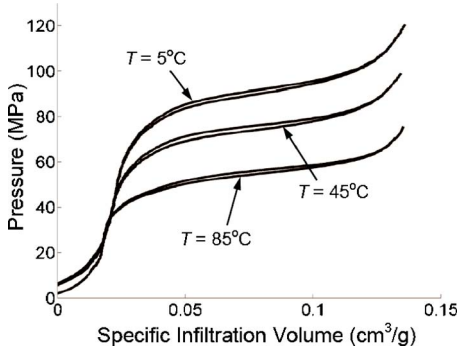

FIG. 2. (Color online) Typical sorption isotherm curves at different temperatures. The curves have been shifted along the horizontal axis.

The mixture of zeolite and water was sealed in a stainless steel container by a piston. By using an Instron machine, the piston was compressed into the container at a constant rate of 0.5 mm/min, resulting in the external load F and the piston displacement δ. The liquid pressure and the liquid volume change were calculated as $P=F/A_0$ and $\Delta V=\delta A_0$, respectively, where $A_0=287$ mm^2 is the cross-sectional area of the container. When the infiltration was completed, the piston was moved out at the same rate. The external force and the piston displacement were measured continuously by a 50KN load cell and a linear variable displacement transducer, respectively. After the pressure was reduced to zero, the loading-unloading cycle was repeated for three to four times. However, since no chances in sorption isotherm curves could be observed, the following discussion will be focused on the first infiltration-defiltration loop.

The system temperature was controlled by an Aldrich DigiTrol II Z28 controlled-temperature bath. The loading-unloading tests were performed at various temperatures of 5, 15, 22, 40, 45, 65, 75, and 85 °C. At each temperature, a reference system of the same structure but containing no zeolite (i.e., the container was filled by pure water) was tested through a similar loading-unloading procedure. Based on the measured pressure-volume curve, the volume change caused by the deformation of testing system, ΔV_0, could be obtained. The infiltration volume was calculated as $\Delta V_{\text{in}}=\Delta V-\Delta V_0$, and the typical sorption isotherm curves are shown in Fig. 2, where the specific infiltration volume is defined as $\Delta V_{\text{in}}/m$, with $m=1$ g being the mass of the zeolite crystals. Figure 3 shows the infiltration pressure and the defiltration pressure.

Through Fig. 2, it can be seen clearly that water infiltration takes place only when the pressure is sufficiently high.

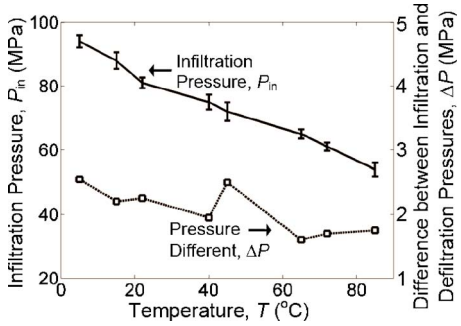

FIG. 3. (Color online) Infiltration pressure and the pressure difference as functions of the temperature.

Initially, when the pressure is relatively low, the system is quite rigid. As pressure increases, water molecules start to enter the nanopores. Consequently, the system volume changes significantly. Once the pressure reaches the critical value, water infiltration becomes pronounced and the effective system compressibility is largely increased. As a result, an infiltration plateau is formed in the sorption isotherm curve. When most of the nanopores are filled, the system is rigid again. The total infiltration volume V_{in} is about 0.12 cm^3/g, smaller than the specific pore volume of the zeolite. Note that V_{in} is quite insensitive to the temperature variation, as it should be.

As the external pressure is lowered, the energy barrier of defiltration is negligible; that is, defiltration occurs at about the same pressure as infiltration. Thus, the defiltration part of the sorption isotherm curve is nearly identical to the infiltration part. In the current study, for the sake of simplicity, the infiltration/defiltration pressure is defined as the pressure at the middle point of the infiltration/defiltration plateau, and the infiltration/defiltration plateau is defined as the part of sorption isotherm curve between two points where the slopes equal to 50% of that of the initial rigid section. According to experimental observations and thermodynamic analyses,[13,14] liquid defiltration in nanopores is strongly dependent on gas phase nucleation and growth. In a nanopore, the infiltration pressure would equal to the defiltration pressure if[13]

$$\frac{2\Delta\gamma}{r}=\frac{2\gamma_{\text{GL}}}{h}+\Delta\mu, \tag{2}$$

where $\Delta\gamma$ is the excess solid-liquid interfacial tension, r is the nanopore size, γ_{GL} is the liquid surface tension, h is the size of gas phase nucleus, and $\Delta\mu$ is the effective energy barrier of liquid-gas phase transformation. If the value of $\Delta\gamma$ is estimated as $p_{\text{in}}r/2$, Eq. (2) can be rewritten as

$$h=\frac{2\gamma_{\text{GL}}}{p_{\text{in}}-\Delta\mu}, \tag{3}$$

with p_{in} being the infiltration pressure. For the system under investigation, as temperature $T=4$ °C, $p_{\text{in}}=94$ MPa, compared with which $\Delta\mu$ is negligible. If γ_{GL} is taken as 72 mJ/g, the required gas phase nucleus size h can be estimated as about 1.6 nm, somewhat larger than but comparable with the nanopore size, which agrees well with the experimental observation that gas "nanobubbles" commonly exist in nanoenvironments.[17]

In the loading process, the work done by the external pressure is converted to the solid-liquid interfacial tension. Upon unloading, since the sorption isotherm curve is nearly nonhysteretic, the release of the stored interfacial energy takes place spontaneously, accompanied by the defiltration of the confined liquid. Hence, as the external load is fully removed, the system configuration is almost identical to that before the test. Such a system can be regarded as a liquid "spring," which, according to the discussion of Soulard *et al.*,[15] can be used for energy storage. In our experiment, it was observed that, when the external pressure was maintained constant at p_{in}, by decreasing temperature the piston could be pushed out; when the temperature was then increased, the piston would move back. The reason is shown clearly in Figs. 2 and 3: as temperature increases, the infiltration pressure, i.e., the pressure at which the liquid spring works, decreases considerably; that is, at an elevated tem-

perature the system becomes "softer," or, equivalently, at a lower temperature the system is "stiffer." As temperature changes from 5 to 85 °C, p_{in} largely decreases from 94 to 56 MPa by nearly 40%, and the p_{in}-T relationship is quite linear, with the temperature sensitivity of $\xi \approx 0.5$ MPa/°C. Therefore, if the pressure is kept constant at the initial p_{in}, as temperature decreases, it becomes insufficient to confine the liquid in the nanopores, and thus the liquid would defiltrate, converting solid-liquid interfacial energy to mechanical work and, vice versa. Such a device is actually a thermally controllable intelligent system, exhibiting a volume memory characteristic. The associated energy density can be calculated as

$$U = \xi V_{in} \Delta T, \tag{4}$$

where ΔT is the temperature variation. If $\Delta T = 80$ °C, U is about 5 J/g, two orders of magnitude higher than that of conventional shape-memory alloys, e.g., Ti–Ni alloys.[18]

The temperature dependence of working pressure should be attributed to the thermal effect on solid-liquid interfacial tension. It has been well known that surface tensions of both liquids and solids are functions of T,[19] and therefore the excess solid-liquid interfacial tension $\Delta\gamma$ is also highly dependent on temperature. In the system under investigation, $\Delta\gamma$ decreases as T increases. As a first-order approximation, the value of $\Delta\gamma$ can be estimated as $p_{in}r/2$. At 5 °C, $\Delta\gamma$ is around 15 mJ/m^2; as T increases to 85 °C, $\Delta\gamma$ decreases quite linearly to 9 mJ/m^2, with the temperature sensitivity of $\zeta \approx 0.07$ mJ/m^2 °C. Note that the energy density can also be assessed as

$$U = \zeta A \Delta T, \tag{5}$$

where $A \approx 900$ m^2/g is the ideal pore surface area. If $\Delta T = 80$ °C, according to Eq. (5), U is about 5.2 J/g, quite close to the result of Eq. (4). Based on Eq. (5), the high energy density of the nanoporous liquid "spring" can be regarded as a result of the amplification effect of A.

According to Eq. (2), as temperature increases, since p_{in} becomes smaller, the required gas phase nucleus size h decreases, i.e., the defiltration is easier. This is in agreement with the measurement result that the difference between infiltration and defiltration pressures tends to decrease with an increasing temperature, as shown by the dashed line in Fig. 3.

In summary, it is validated experimentally that nanoporous materials of nonhysteretic sorption isotherm curves can be employed to develop volume memory systems. Under the working pressure, as temperature changes, the effective wettability varies, and thus the liquid tends to either infiltrate into or defiltrate out of the nanopores, resulting in a thermally controllable actuation behavior. Due to the large specific surface area, the wettability variation is greatly amplified. Consequently, the energy density can be much higher than that of conventional smart solids.

The experimental work and the data analysis were supported by The Air Force Office of Scientific Research under Grant No. FA9550-06-1-0181, for which the authors are grateful to B.-L. Lee. The materials preparation was supported by The National Science Foundation under Grant No. CMS-0621550, for which the authors are grateful to K. J. Hsia. Special thanks are also due to D. K. Panchal for the help with preparing the experimental devices.

[1] S. Polarz and B. Smarsly, J. Nanosci. Nanotechnol. **2**, 581 (2002).
[2] A. Laouir, L. Luo, D. Tondeur, T. Cachot, and P. Le Goff, AIChE J. **49**, 764 (2003).
[3] A. Dabrowski, Adv. Colloid Interface Sci. **93**, 135 (2001).
[4] S. H. Pandey and R. S. Chauhan, Prog. Polym. Sci. **26**, 853 (2001).
[5] V. Eroshenko, R. C. Regis, M. Soulard, and J. Patarin, C. R. Phys. **3**, 111 (2002).
[6] T. Martin, B. Lefevre, D. Brunel, A. Galarneau, F. Di Renzo, F. Fajula, P. F. Gobin, J. F. Quinson, and G. Vigier, Chem. Commun. (Cambridge) **2002**, 24.
[7] X. Kong and Y. Qiao, Appl. Phys. Lett. **86**, 151919 (2005).
[8] F. B. Surani, X. Kong, D. B. Panchal, and Y. Qiao, Appl. Phys. Lett. **87**, 163111 (2005).
[9] X. Kong, F. B. Surani, and Y. Qiao, J. Mater. Res. **20**, 1042 (2005).
[10] A. Han and Y. Qiao, J. Am. Chem. Soc. **128**, 10348 (2006).
[11] Y. Qiao and X. Kong, Phys. Scr. **71**, 27 (2005).
[12] V. D. Borman, A. M. Grekhov, and V. I. Troyan, J. Exp. Theor. Phys. **91**, 170 (2000).
[13] A. Han, X. Kong, and Y. Qiao, J. Appl. Phys. **100**, 014308 (2006).
[14] B. Lefevre, A. Saugey, J. L. Barrat, L. Bocquet, E. Charlaix, P. F. Gobin, and G. Vigier, J. Chem. Phys. **120**, 4927 (2004).
[15] M. Soulard, J. Patarin, V. Eroshenko, and R. Regis, Stud. Surf. Sci. Catal. **154**, 1830 (2004).
[16] S. M. Auerbach, K. A. Carrado, and P. K. Dutta, *Handbook of Zeolite Science and Technology* (CRC, Boca Raton, FL, 2003).
[17] R. Kimmich, Chem. Phys. **284**, 253 (2002).
[18] Z. G. Wei, R. Sandstrom, and S. Miyazaki, J. Mater. Sci. **33**, 3743 (1998).
[19] J. M. Howe, *Interface in Materials* (Wiley, New York, 1997).